

Statistical Properties of a Blazar Sample and Comparison of HBLs, LBLs and FSRQs

Li-Sheng Mao^{1,2}, Guang-Zhong Xie^{1,3}, Jin-Ming Bai¹ and Hong-Tao Liu^{1,2}

¹ Yunnan Observatory, National Astronomical Observatories, Chinese Academy of Sciences, Kunming 650011; maolisheng1981@126.com

² Graduate University of Chinese Academy of Sciences, Beijing 100049

³ Yunnan Astrophysics Center, Yunnan University, Kunming, 650091

Received 2005 March 19; accepted 2005 June 3

Abstract Making use of the 2MASS Data Release, we have searched for near-infrared (JHK) counterparts to 268 blazars from Donato et al. and obtained 238 counterparts within 5'' in the area covered by 2MASS. It provides us a sample with infrared data several times larger than the previous one of the same kind. Based on our sample and the sample by Donato et al., we have compared in detail the properties of HBLs, LBLs and FSRQs from five aspects and found that HBLs are significantly different from LBLs and FSRQs while LBLs are not obviously different from FSRQs. Our results strongly support the division of BL Lac objects into the high-frequency peaked (HBL) and low-frequency peaked (LBL) objects introduced by Padovani & Giommi and show that HBLs and LBLs are two kinds of blazar having different physical properties.

Key words: BL Lacertae objects: general— infrared: galaxies — methods: statistical

1 INTRODUCTION

Blazars are compact, flat spectrum radio sources with highly variable and polarized nonthermal continuum emission extending up to X-ray and often γ -ray frequencies (Fugmann 1988; Urry & Padovani 1995; Angle & Stockman 1980; Xie et al. 2004a, 2004b; Bregman et al. 1990; Sillanpaa et al. 1991). In some cases their emission lines are very weak or absent (equivalent width $< 5 \text{ \AA}$), a property which defines the subclass of blazars, the BL Lac objects. Other blazars have broad emission lines similar to those of normal quasars, depending on how they were identified. These are known as optically violently variable quasars (OVVs), highly polarized quasars (HPQs), flat spectrum radio quasars (FSRQs), or core-dominant radio quasars (CDQs). Traditionally, BL Lac objects discovered in radio sky surveys are called radio-selected BL Lac objects (RBLs), and those discovered in X-ray sky surveys are called X-ray-selected BL Lacs (XBLs). Recently a new classification has been introduced, based on the fact that the peak wavelength of the

synchrotron luminosity in blazars is anticorrelated with the ratio of X-ray to radio flux. On this basis, Padovani & Giommi (1995) divided BL Lac objects into high-frequency peaked (HBL) and low-frequency peaked (LBL) objects, according as α_{rx} (from 5 GHz to 1 keV) is < 0.75 (Urry & Padovani 1995) or 0.80 (Sambruna et al. 1996). In this scheme, most (but not all) RBLs are LBLs and most (but not all) XBLs are HBLs.

In 1994, Giommi and Padovani made the following point (Giommi & Padovani 1994): when the EMSS and 1 Jy samples were the only sizable BL Lac samples available, the division between XBLs and RBLs was clear-cut. However, with the advent of all-sky X-ray surveys, like the Slew survey (Perlman et al. 1996) and especially the ROSAT All-Sky Survey (RASS, Voges et al. 1996 and Brinkmann et al. 1995), this was no longer the case. Those surveys include many BL Lacs previously selected at radio frequencies, which could now be classified either as XBLs or as RBLs. So it is clear that a distinction based on the observing band is not physical and is bound to fail when deeper radio and X-ray surveys are available (Padovani 1999). On the other hand, the classification of HBLs and LBLs is based on a physical difference and not on the observing band: in the HBLs the X-ray emission is produced by synchrotron emission, whereas in the LBLs, the X-ray is dominated by the inverse Compton component (Bondi et al. 2001). The change of perspective from XBLs/RBLs to HBLs/LBLs has had important implications for the accelerating jet model and has spurred a strong interest in the study of the physical parameters underlying the emission process in BL Lacs. In a word, the classification of HBLs and LBLs is better and has more physical significance than the classification of XBLs and RBLs.

Therefore, searching for connections between the different types of blazars, namely, HBLs, LBLs and FSRQs, will substantially advance our understanding of the fundamental nature of blazars. This topic has been studied by many authors (Padovani & Giommi 1995; Giommi et al. 1990; Lamer, Brunner & Staubert 1996; Sambruna et al. 1996; Stecker et al. 1996; Wolter, Comastri & Ghisellini 1998; Xie et al. 2001a, 2001b, 2003, 2004c; D’Elia & Cavalitre 2001; Böttcher & Dermer 2002). The properties of LBLs are systematically different from those of HBLs: (1) These two subclasses occupy different regions on the $\alpha_{ro} - \alpha_{ox}$ plane, which shows the indicative spectral energy distribution; (2) There exist correlations between the minimum soft X-ray flux and radio flux, and between the radio and optical fluxes for HBLs, but not for LBLs; (3) The observed peak of emitted power typically locates at millimeter/IR for LBLs and at UV/soft X-ray wavelength for HBLs; (4) FSRQs, HBLs and LBLs are mixed together in the $\alpha_{ox} - \alpha_{x\gamma}$ plane but are located in separate regions in the diagram of composite spectral indices $\alpha_{xox} - \alpha_{\gamma x\gamma}$. The LBLs bridge the gap between the FSRQs and HBLs; (5) HBLs have lower polarization and lower redshift than LBLs.

Up to now, the relationship between BL Lacs and FSRQs is unclear while of great interest. The blazar-like nonthermal continuum and properties such as rapid variability and polarization are common to both FSRQs and BL Lacs, which nominally differ only in their emission line properties. An evolutionary link between them may explain the correlation of broadband properties with redshift (Vagnetti, Cavaliere & Giallongo 1991), although this suggestion was based on few (four) BL Lacs which were later found to have broad emission lines. It does not appear to be supported by the broadband and emission-line properties of larger samples (Padovani 1992). Continuity of the radio and X-ray luminosity functions also suggests a continuity of some kind between RBLs and FSRQs (Maraschi & Rovetti 1994).

In this paper, we will study the differences between HBLs and LBLs, HBLs and FSRQs, LBLs and FSRQs, through multi-wave band flux correlations and spectral energy distribution, especially the differences of HBLs, LBLs and FSRQs in the near-infrared spectrum. The data selection and analysis are described in Section 2. In Section 3 we will compare the physical properties of HBLs, LBLs and FSRQs from five aspects. A discussion and results are summarized in Section 4.

2 DATA DESCRIPTION

Active galactic nuclei (AGNs) have been studied for several decades, but our understanding of many aspects of AGNs is still rudimentary. Our inability to definitively understand AGNs to date may be due to selection effects. Most high luminosity AGNs have been selected using their rest-frame ultraviolet through optical colors in optically magnitude-limited samples. It is therefore almost certain that dust obscuration has masked some portions of the AGNs found by their ultraviolet-optical colors which are less dusty than the truly typical AGNs (Webster et al. 1995; Baker 1997; Wills & Hines 1997). This bias against dust-obscured objects can affect our understanding of the AGNs, in particular their connection to their host galaxies and nuclear environments. A sample selected only by near-infrared magnitude is an excellent way to reduce any bias against dust-obscured objects. The Two-Micron All-Sky Survey (2MASS, Skrutskie et al. 1997) has now made it feasible to select samples of AGNs in the near-infrared (NIR). To provide a sample of blazars with homogeneous infrared data, we searched for near-infrared counterparts to 268 blazars from the sample by Donato et al. (2001).

The internal errors of 2MASS astrometry are, on average, $0.3''$ for our detection of blazars, so the uncertainty in the astrometric matching is dominated by the errors in the blazar coordinates. In addition, most of the blazars in the sample by Donato et al. (2001) have optical positions which are accurate to $< 1''$ or have similarly accurate radio positions. Based on the accurate position identification, we have acquired 238 counterparts within $5''$ within the area covered by the 2MASS Data Release. Among these only two blazars (0607+7108 and 2319+161) have two counterparts within $5''$. Thus we compiled a large sample of blazars containing 118 HBLs, 60 LBLs and 60 FSRQs which is much larger than any previous such sample with infrared data. Although the sample is not complete, it is the largest database of this kind and we think it is representative of the entire blazar class. The large number of sources in each subcategory of blazars can be used to compare the properties of HBLs, LBLs and FSRQs.

The infrared data are listed in Tables 5, 6, 7¹ with the following headings: column (1), IAU name; column (2), the right ascension (Deg); column (3), the declination (Deg); column (4), reference for the position in columns (2) and (3); column (5), the distance between the position of sources and the counterparts in the 2MASS (arcsec); columns (6) and (7), the right ascension and declination of the counterparts in 2MASS (Deg); column (8), the J magnitude; column (9), the uncertainty in the J magnitude; column (10), the H magnitude; column (11), the uncertainty in the H magnitude; column (12), the K_s magnitude; column (13), the uncertainty in the K_s magnitude; column (14), the distance between the counterpart and its associated optical source.

3 COMPARISON BETWEEN LBLs, HBLs AND FSRQs

3.1 JHK Correlation

We have checked the $J - H$, $H - K$ and $J - K$ correlations. The main conclusions are listed in Table 1 and displayed in Figure 1. From the results of the correlation analysis, we found that strong correlations between $J - H$ and $J - K$ and between $H - K$ and $J - K$ are shown by all three samples (the HBLs, LBLs and FSRQs) and by their combined sample. However, as regards the correlation between $J - H$ and $H - K$, the LBLs and FSRQs show no correlation, while the 118 HBLs show quite a strong negative one with correlation coefficient $r = -0.406$ and chance probability 4.971×10^{-6} (discarding the more distant of the two counterparts which both of 0607+7108 and 2319+161 have). Fan et al. (1998) have examined the correlations between $J - H$, $H - K$ and $J - K$ for the individual BL Lacertae and found that there are strong

¹ Tables 5, 6 and 7 are only available in electronic form at http://www.chjaa.org/2005_5_5.htm.

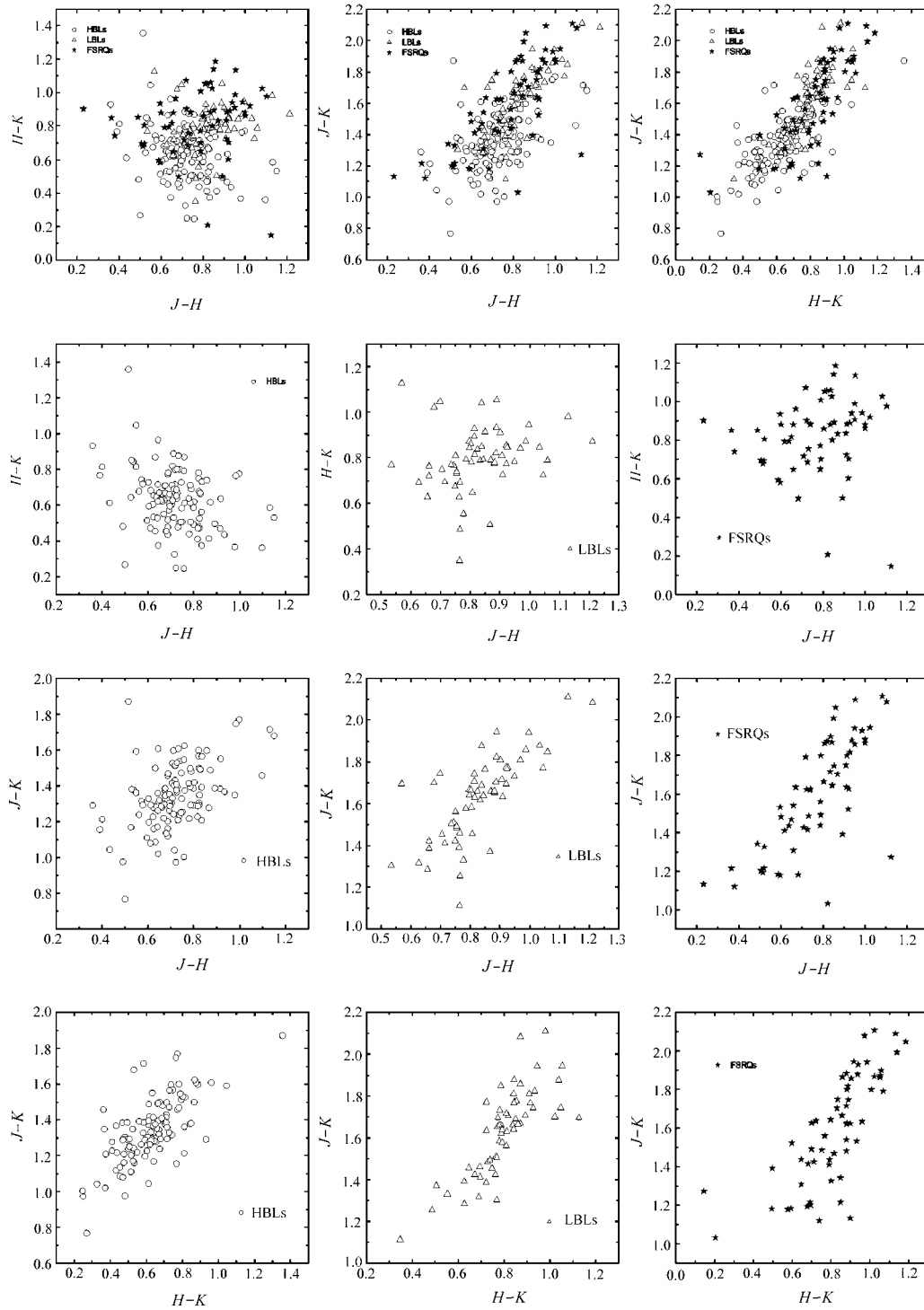


Fig. 1 $(J - H)$ vs $(H - K)$; $(J - H)$ vs $(J - K)$; $(H - K)$ vs $(J - K)$. The empty circles represent HBLs, empty triangles LBLs, and stars FSRQs.

Table 1 *JHK* correlations. Here r denotes the Pearson's coefficient and p the chance probability.

| Type | $(J - H) - (H - K)$ | $(J - H) - (J - K)$ | $(H - K) - (J - K)$ |
|-----------------|---|--|---|
| HBLs | $r = -0.406$ $p = 4.971 \times 10^{-6}$ $N = 118$ | $r = 0.468$ $p = 9.195 \times 10^{-8}$ $N = 118$ | $r = 0.688$ $p = 7.205 \times 10^{-18}$ $N = 118$ |
| LBLs | $r = 0.179$ $p = 0.171$ $N = 60$ | $r = 0.748$ $p = 6.22 \times 10^{-12}$ $N = 60$ | $r = 0.787$ $p = 9.451 \times 10^{-14}$ $N = 60$ |
| FSRQs | $r = 0.108$ $p = 0.411$ $N = 60$ | $r = 0.731$ $p = 3.383 \times 10^{-11}$ $N = 60$ | $r = 0.757$ $p = 2.468 \times 10^{-12}$ $N = 60$ |
| HBLs+LBLs+FSRQs | $r = 0.064$ $p = 0.326$ $N = 238$ | $r = 0.661$ $p = 2.89 \times 10^{-31}$ $N = 238$ | $r = 0.791$ $p \approx 0$ $N = 238$ |

correlations between $J - H$ and $J - K$ and between $H - K$ and $J - K$ but no correlation between $J - H$ and $H - K$. They thought it is because $J - K$ has a wider distribution than $J - H$ or $H - K$. That $J - H$ and $H - K$ concentrate in a small region dilutes the correlation. Another reason probably comes from the fact that the spectrum deviates from the power-law. Fan & Lin (1999) found there are mutual correlations between any two of the color indices $J - H$, $H - K$ and $J - K$ when the averaged color indices are taken into account for 40 LBLs: $(H - K) = 1.44(J - H) - 0.41$ with $r = 0.80$ and $p = 4.4 \times 10^{-7}$; $(J - K) = 2.26(J - H) - 0.28$ with $r = 0.90$ and $p = 6.3 \times 10^{-11}$; $(J - K) = 1.62(H - K) + 0.33$ with $r = 0.93$ and $p = 6.1 \times 10^{-13}$. Gear (1993) presented a single-epoch infrared photometry of two complete samples of BL Lacertae objects, one radio-selected (RBLs) and one X-ray-selected (XBLs) and found that the RBLs fall into two distinct groups on the $(J - H) - (H - K)$ plane. From figure 1 in Gear (1993), we can also find that for 20 XBLs (HBLs) $J - H$ is strongly anticorrelated with $H - K$ (the correlation coefficient $r = -0.76$ and the chance probability $p = 1.09 \times 10^{-4}$) while for 35 RBLs (LBLs), $J - H$ is very weakly correlated with $H - K$ ($r = 0.42$ and $p = 0.01$), which is consistent with our results. The positive correlation between $J - H$ and $H - K$ for 40 LBLs of Fan & Lin (1999), the negative correlations between $J - H$ and $H - K$ for 118 HBLs in our sample, and 20 HBLs in Gear (1993) point to some essential differences between HBLs and LBLs, in their near-infrared spectral energy distribution.

3.2 NEAR-INFRARED SPECTRUM COMPARISON

We have compared in detail the averaged color indices of HBLs, LBLs and FSRQs. The results are as follows: for HBLs, $\langle J - H \rangle = 0.720 \pm 0.012$, $\langle H - K \rangle = 0.632 \pm 0.015$, and $\langle J - K \rangle = 1.347 \pm 0.016$; for LBLs, $\langle J - H \rangle = 0.833 \pm 0.017$, $\langle H - K \rangle = 0.799 \pm 0.018$, and $\langle J - K \rangle = 1.632 \pm 0.026$; for FSRQs, $\langle J - H \rangle = 0.772 \pm 0.024$, $\langle H - K \rangle = 0.824 \pm 0.025$, and $\langle J - K \rangle = 1.596 \pm 0.037$; for LBLs + FSRQs, $\langle J - H \rangle = 0.803 \pm 0.015$, $\langle H - K \rangle = 0.811 \pm 0.015$, and $\langle J - K \rangle = 1.614 \pm 0.023$. In order to characterize the shape of blazar spectral energy distribution, we can consider the composite spectral index (Ledden & O'Dell 1985), which is defined as:

$$\alpha_{12} = -\frac{\log(F_1/F_2)}{\log(\nu_1/\nu_2)}, \quad (1)$$

Table 2 Student's t-test results. The numbers in the table are the Student's-test significance level probability. Small values mean that the two distributions have significantly different means (see Press et al. 1992).

| Type | α_{JH} | α_{HK} | α_{JK} |
|------------|------------------------|-------------------------|-------------------------|
| HBLs-LBLs | 2.201×10^{-7} | 9×10^{-11} | 6.578×10^{-18} |
| HBLs-FSRQs | 3.310×10^{-2} | 4.376×10^{-11} | 2.126×10^{-11} |
| LBLs-FSRQs | 3.891×10^{-2} | 0.421 | 0.425 |

Table 3 K-S test results. We have used one-dimensional Kolmogorov-Smirnov test to compare the distribution of three infrared composite spectral indices α_{JH} , α_{HK} and α_{JK} of HBLs, LBLs and FSRQs (the K-S test probabilities are listed in column 2-4 of the following table). Moreover, we have used two-dimensional K-S test to compare the distribution of the three composite spectral indices (the two-dimensional K-S test probabilities are listed in column 5-7 of the following table). Small values of the K-S test probability mean that the two distributions are significantly different (see Press et al. 1992, page 617–620 and page 640–643).

| Type | α_{JH} | α_{HK} | α_{JK} | $\alpha_{JH} - \alpha_{HK}$ | $\alpha_{JH} - \alpha_{JK}$ | $\alpha_{HK} - \alpha_{JK}$ |
|------------|------------------------|-------------------------|-------------------------|-----------------------------|-----------------------------|-----------------------------|
| HBLs-LBLs | 1.542×10^{-7} | 3.503×10^{-12} | 1.155×10^{-12} | 7.819×10^{-11} | 2.144×10^{-9} | 2.959×10^{-11} |
| HBLs-FSRQs | 8.294×10^{-4} | 1.342×10^{-10} | 8.018×10^{-9} | 3.303×10^{-8} | 3.261×10^{-7} | 7.243×10^{-8} |
| LBLs-FSRQs | 3.873×10^{-2} | 1.261×10^{-2} | 0.476 | 2.931×10^{-3} | 2.436×10^{-2} | 1.395×10^{-2} |

where F_1 and F_2 are the flux densities at frequencies ν_1 and ν_2 , respectively. For all the objects in our sample, we compute the averaged composite spectral indices: α_{JH} , α_{HK} and α_{JK} . For 118 HBLs: $\langle \alpha_{JH} \rangle = 0.793 \pm 0.041$, $\langle \alpha_{HK} \rangle = 0.543 \pm 0.051$, $\langle \alpha_{JK} \rangle = 0.669 \pm 0.027$. For 60 LBLs, $\langle \alpha_{JH} \rangle = 1.171 \pm 0.055$, $\langle \alpha_{HK} \rangle = 1.118 \pm 0.060$, $\langle \alpha_{JK} \rangle = 1.145 \pm 0.044$. For 60 FSRQs, $\langle \alpha_{JH} \rangle = 0.968 \pm 0.080$, $\langle \alpha_{HK} \rangle = 1.202 \pm 0.085$, $\langle \alpha_{JK} \rangle = 1.084 \pm 0.061$. Obviously, all averaged composite spectral indices of HBLs are smaller than those of LBLs and FSRQs. We use the Student's t-test to test whether or not the averaged composite spectral indices of the three subclasses are the same. The results are listed in Table 2, which show that the averaged composite indices of HBLs are significantly different from those of LBLs and FSRQs, but the averaged composite spectral indices of LBLs are not demonstrably different from those of FSRQs and nearly have the same means with those of FSRQs, especially for α_{HK} and α_{JK} (see Fig. 2). Furthermore, using the one dimensional Kolmogorov-Smirnov (K-S) test and two-dimensional K-S test (see Press et al. 1992) for the distribution of the composite spectral indices gives almost identical results (see Table 3). The HBLs have significantly flatter infrared composite spectral indices than the LBLs and FSRQs, and in contrast, the distributions and means of α_{JH} , α_{HK} and α_{JK} for LBLs and FSRQs are not demonstrably different.

3.3 Luminosity Comparison

In this part we compare the K_s -band luminosities of the three subclasses. All K_s -band densities are K-corrected according to $F_v = F_v^{\text{obs}}(1+z)^{\alpha-1}$, where α is the spectral index ($F_v \propto \nu^{-\alpha}$). We assume a near-infrared spectral index $\alpha = 0.5$ for HBLs and $\alpha = 1$ for LBLs and FSRQs (Falomo et al. 1993), and a Hubble constant of $H_0 = 50 \text{ km s}^{-1} \text{ Mpc}^{-1}$ and $q_0 = 0.5$. The averaged luminosities of the three subclasses are respectively: $\langle \nu L_{\nu_K} \rangle_{\text{HBL}} = 10^{44.611} \text{ erg s}^{-1}$,

$\langle vL_{\nu_K} \rangle_{\text{LBL}} = 10^{45.491} \text{ erg s}^{-1}$ and $\langle vL_{\nu_K} \rangle_{\text{FSRQ}} = 10^{45.987} \text{ erg s}^{-1}$. The distribution of K_s -band luminosities (see Fig. 3) shows a continue variation in the three subclasses of blazar: HBLs are the least powerful sources, and FSRQs are the most luminous objects, and LBLs are between the two. The K-S test results are as follows: HBLs vs LBLs, $p = 9.926 \times 10^{-17}$; HBLs vs FSRQs, $p = 1.902 \times 10^{-22}$; LBLs vs FSRQs, $p = 1.802 \times 10^{-3}$; HBLs vs (LBLs + FSRQs), $p = 7.933 \times 10^{-21}$. Student's t-test results are as follows: HBLs vs LBLs, $p = 1.961 \times 10^{-20}$; HBLs vs FSRQs, $p = 1.524 \times 10^{-36}$; LBLs vs FSRQs, $p = 1.339 \times 10^{-4}$; HBL vs (LBLs + FSRQs), $p = 2.785 \times 10^{-23}$. These results show that HBLs have a significantly different distribution and mean of near-infrared luminosity from LBLs and FSRQs. The K_s -band luminosities of FSRQs and LBLs are somewhat similar, while HBLs are less luminous by a factor 10. Donato et al. (2001) have calculated the radio, optical and X-ray luminosities of the HBLs, LBLs and FSRQs and also found that HBLs are the least powerful sources, and FSRQs are the most luminous objects in the three subclasses of blazar. Their results are consistent with our infrared results.

3.4 Correlation between Luminosity and Spectral Index

Fossati et al. (1998) have computed average spectral energy distributions (SEDs) from radio to γ -ray for a large blazar sample and found that the synchrotron peak frequency, $\nu_{\text{peak, sync}}$, decreases with increasing radio, γ -ray and synchrotron peak luminosities and with steeper composite spectral indices α_{rx} , α_{ro} . In fact, some authors (Maraschi et al. 1995; Comastri et al. 1995, 1997; Qin et al. 1999; Dong, Mei & Liang 2002) have suggested that the position of the synchrotron peak could be derived from the values of composite spectral indices. Sambruna et al. (1996) found that the position of the synchrotron peak frequency, $\log \nu_{\text{peak, sync}}$, is linked to the bolometric luminosity. For more luminous objects, the peak of the synchrotron power is located at lower frequencies. From the above facts, we can conclude that the peak frequency is strongly correlated with the luminosity and with the composite spectral indices α_{rx} and α_{ro} . Is there strong correlation between the luminosity and the composite spectral indices? In the following part, we will investigate the correlation between the luminosity and the composite spectral index α_{rx} .

Mei et al. (2002) have studied the correlation between luminosity and the composite spectral index α_{rx} and found that the radio luminosity can well distinguish HBLs and LBLs, while the optical and X-ray luminosities cannot. The sample of Mei et al. (2002) includes 25 HBLs and 27 LBLs; our sample is several time larger and enables us to test the conclusion that we can use the radio luminosity but not the optical and X-ray luminosities as a classificatory criterion of BL Lacertae objects and to investigate the correlation of luminosity and the composite spectral index α_{rx} . Using the radio data of Donato et al. (2001) and based on our newly compiled sample (including 118 HBLs, 60 LBLs and 60 FSRQs), we now consider the relationship between radio luminosity and the composite spectral index α_{rx} . We plot $\log v L_{\nu_R}$ versus α_{rx} in Figure 4, which shows that the radio luminosity increases as the composite spectral index increases. In this figure, four different regions are marked out by the lines $\alpha_{\text{rx}} = 0.75$ and $\log v L_{\nu_R} = 42.20 \text{ erg s}^{-1}$; 78.3% LBLs (47 of 60 LBLs) are located in the upper-right region; 94.1% HBLs (111 of 118 HBLs) are inside the lower-left region; six LBLs are in the lower-right region and five LBLs are in the upper-left region and two LBLs are in the lower-left region; seven HBLs are in the upper-left region. These results differ somewhat from the result obtained by Mei et al. (2002) based on a smaller sample; on the whole our results support the thesis that radio luminosity can be used to distinguish HBLs and LBLs and as a classificatory criteria of BL Lacertae objects, because most of HBLs have $\alpha_{\text{rx}} < 0.75$ and $\log v L_{\nu_R} < 42.20 \text{ erg s}^{-1}$ and most of LBLs have $\alpha_{\text{rx}} > 0.75$ and $\log v L_{\nu_R} > 42.20 \text{ erg s}^{-1}$. Moreover, from Figure 4, we can find that most of FSRQs (54 of 60 FSRQs) are located in the same region as the LBLs, with $\alpha_{\text{rx}} > 0.75$ and $\log v L_{\nu_R} > 42.20 \text{ erg s}^{-1}$. This indicates that the radio luminosity can

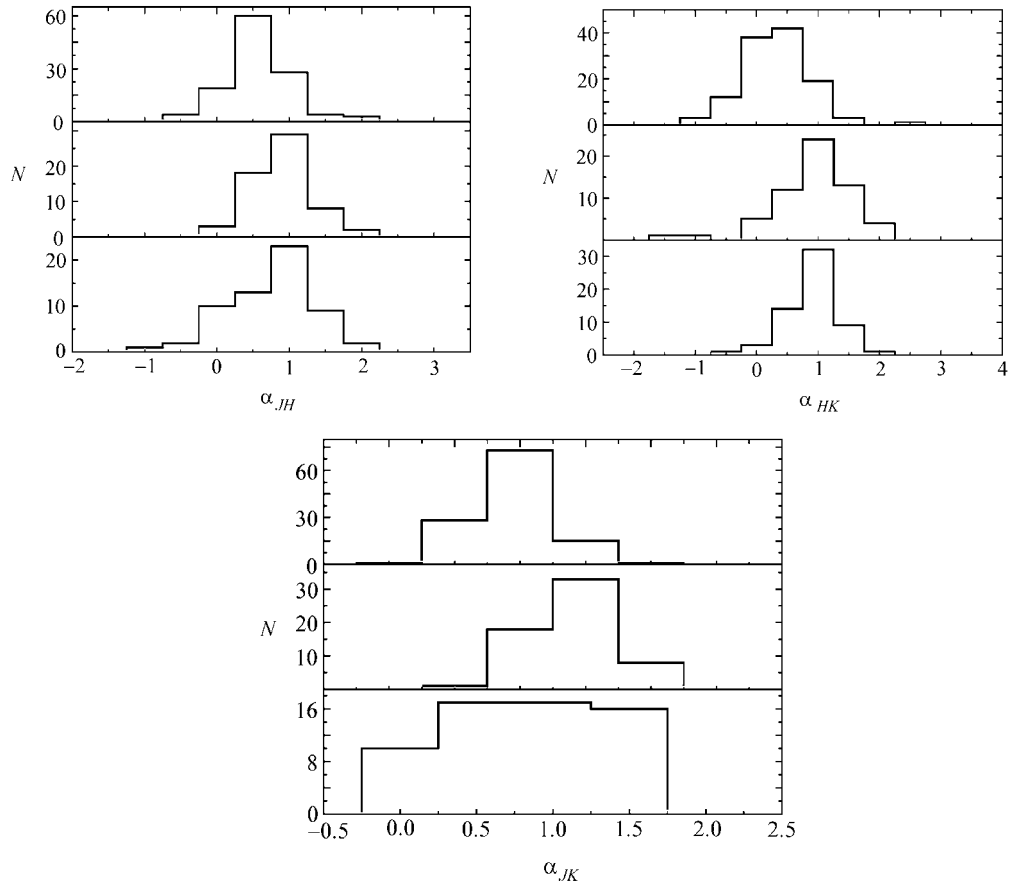


Fig. 2 Distribution of the composite spectral index α_{JH} , α_{HK} and α_{JK} . The top graphs are for HBLs, the middle graphs are for LBLs and the bottom graphs are for FSRQs.

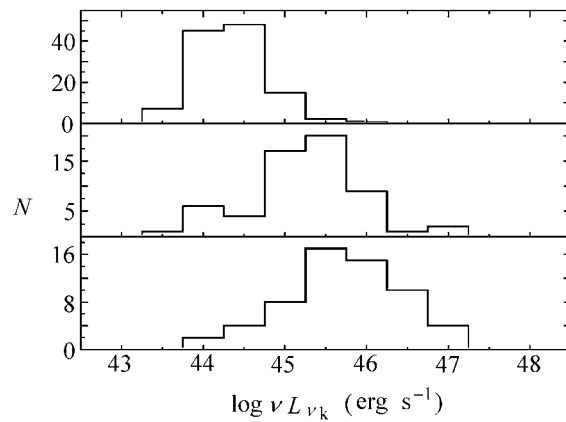


Fig. 3 Distribution of the K_s -band luminosities of the three subclasses. The top graph is for HBLs, the middle is for LBLs and the bottom is for FSRQs. The luminosities have been K-corrected and calculated with a Hubble constant of $H_0 = 50 \text{ km s}^{-1} \text{ Mpc}^{-1}$ and $q_0 = 0.5$.

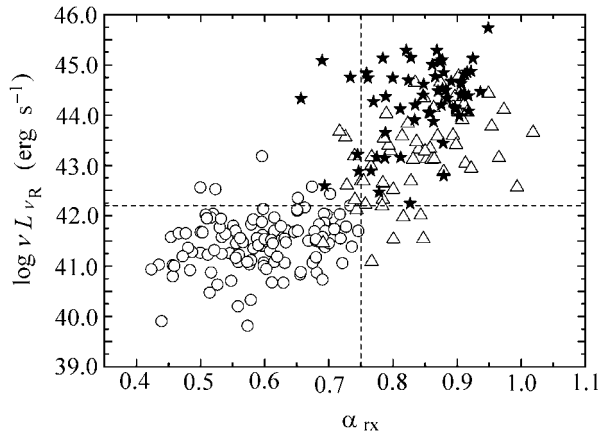


Fig. 4 A plot of $\log v L_{\nu_R} - \alpha_{rx}$ for the total sample. The empty circles represent HBLs, empty triangles LBLs and stars FSRQs. The vertical dashed line is $\alpha_{rx} = 0.75$, and the horizontal dashed line is $\log v L_{\nu_R} = 42.20 \text{ erg s}^{-1}$.

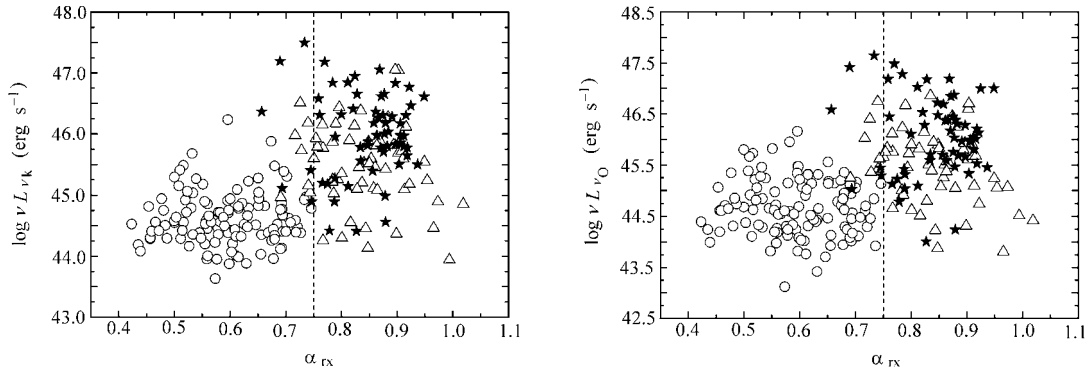


Fig. 5 A plot of $\log v L_{\nu_K} - \alpha_{rx}$ and $\log v L_{\nu_O} - \alpha_{rx}$ for the total sample. The empty circles represent HBLs, empty triangles LBLs and stars FSRQs. The vertical dashed lines are $\alpha_{rx} = 0.75$.

also distinguish HBLs and FSRQs well. Donato et al. (2001) used the K-S test to compare the radio, optical and X-ray luminosities of HBLs and LBLs, and we have used the K-S test to compare the near-infrared luminosities. For the radio, near-infrared, optical and X-ray bands the K-S probabilities are respectively 7×10^{-19} , 9.926×10^{-17} , 2×10^{-7} and 0.6. Therefore, HBLs are most significantly different from LBLs in the radio band, and from radio to X-ray band the discrimination of luminosity between HBLs and LBLs becomes increasingly weaker. From Figures 5 and 6 we can find that the infrared, optical and X-ray luminosities cannot distinguish HBLs and LBLs well, especially the X-ray luminosity.

HBLs have many different properties to LBLs, especially as regards the origin of X-rays: the X-rays in HBLs are mainly from synchrotron emission whereas those in LBLs are dominated by

the inverse Compton component. So it is of great importance to study the correlation between the X-ray luminosity and the composite spectral index α_{rx} . In the following, we present a detailed study of the correlation between the X-ray luminosity $\log v L_{v_X}$ and α_{rx} for HBLs, LBLs and FSRQs (see Fig. 6). The X-ray luminosities are calculated from the data of Donato et al (2001). It is necessary to point that for the sources which have more than one X-ray flux we take an average after the K-correction. For 118 HBLs, there is a very strong negative correlation between $\log v L_{v_X}$ and α_{rx} :

$$\log v L_{v_X} = (-5.941 \pm 0.551)\alpha_{\text{rx}} + 49.002 \pm 0.338, \quad (2)$$

with $r = -0.683$ and $p = 1.643 \times 10^{-17}$. For 60 LBLs, there is a correlation:

$$\log v L_{v_X} = (-2.163 \pm 1.299)\alpha_{\text{rx}} + 47.129 \pm 1.010, \quad (3)$$

with $r = -0.218$ and $p = 0.095$. Obviously, there is no correlation between the X-ray luminosity and the composite spectral index α_{rx} for LBLs. For 60 FSRQs, there is a correlation:

$$\log v L_{v_X} = (-3.525 \pm 1.455)\alpha_{\text{rx}} + 49.230 \pm 1.264, \quad (4)$$

with $r = -0.34$ and $p = 0.008$. From the result we can find that a very weak correlation exists between the X-ray luminosity and the composite spectral index for 60 FSRQs.

3.5 Flux Correlation Of Multi-Wave Band Emission

Donato et al. (2001) collected 421 spectra of 268 blazars, which were observed in the X-ray band and the slope of which the X-ray spectrum is available, and include the radio, optical and X-ray data. Besides, we have collected the JHK magnitudes of those blazars from the 2MASS database if supported. In the following, we will study the multi-wave band flux correlations. For the radio fluxes, average values are used when there are more than one observation; the optical fluxes reported in the NED database are calculated using the indicated magnitude de-reddened with the galactic extinction A_B as reported in the NED database. When we found only the 0.1–2.4 keV and/or 2–10 keV integrated fluxes in the literature, we derived the fluxes at 1 keV using the corresponding X-ray spectral index (Donato et al. 2001). All flux densities are K-corrected according to $F_v = F_v^{\text{obs}}(1+z)^{\alpha-1}$, where α is the spectral index ($F_v \propto v^{-\alpha}$). We assumed a radio spectral index $\alpha = 0$ for all blazars; an optical and near-infrared spectral index $\alpha = 0.5$ for HBLs and $\alpha = 1$ for the LBLs and FSRQs (Falomo et al. 1993; Donato et al. 2001). The correction for blazars with unknown redshift was computed using the average redshift appropriate to each subclass (i.e. $\langle z \rangle_{\text{HBL}} = 0.249$, $\langle z \rangle_{\text{LBL}} = 0.457$ and $\langle z \rangle_{\text{FSRQ}} = 1.265$). For the X-ray band, many sources have more than one X-ray flux. Then we first K-corrected every flux according to its spectral index and then computed the mean of the K-corrected fluxes as the value to be used in the linear regression. The correlation analysis results are given in Table 4 and Figures 7, 8 and 9. The principal results are

1. There are very strong correlations between $\log F_K$ and $\log F_O$ for HBLs, LBLs and FSRQs. The correlation coefficients are respectively 0.719, 0.758 and 0.733 and the chance probabilities are all less than 10^{-4} .
2. For HBLs and FSRQs there are strong correlations between $\log F_R$ and $\log F_K$, but a very weak or no correlation between $\log F_R$ and $\log F_K$ for LBLs.
3. For HBLs and FSRQs there are strong correlations between $\log F_R$ and $\log F_O$, but no correlation between $\log F_R$ and $\log F_O$ for LBLs.
4. There are strong correlations between $\log F_X$ and $\log F_R$, between $\log F_X$ and $\log F_K$ and between $\log F_X$ and $\log F_O$ for HBLs, LBLs and FSRQs. Moreover, from the linear regression results, we can find that the relationships between the X-ray flux and the three lower-frequency band fluxes are much closer for HBLs than for LBLs and FSRQs.

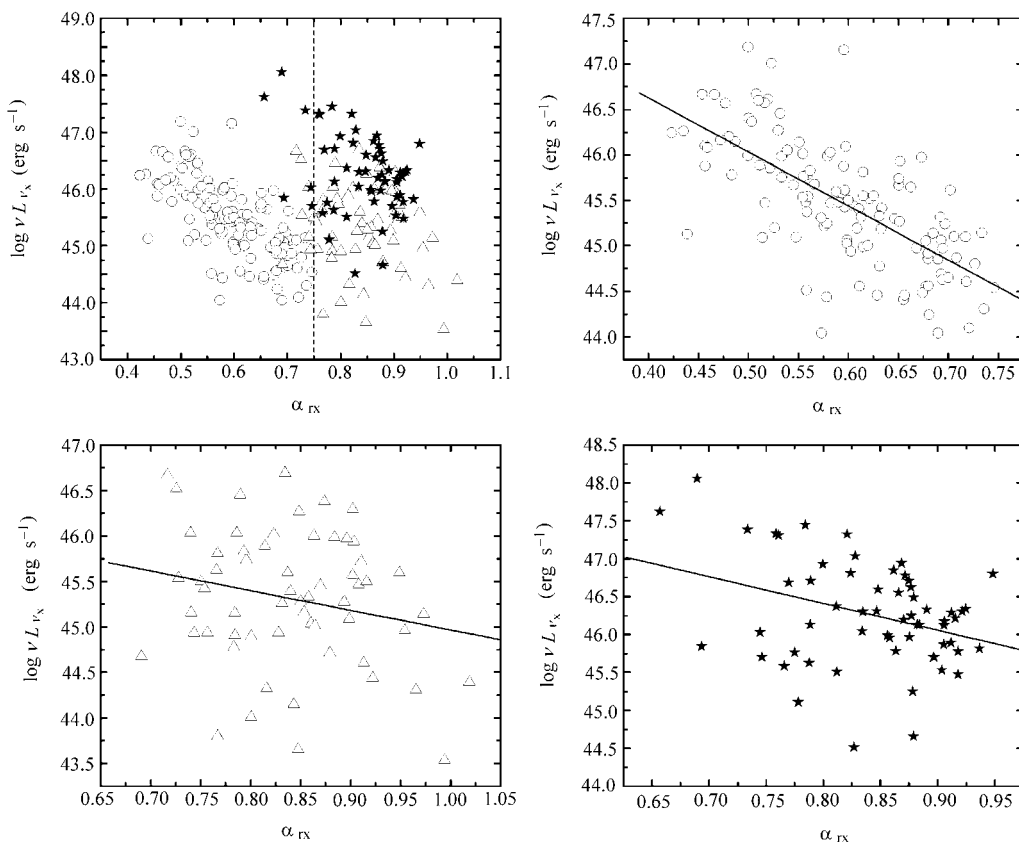


Fig. 6 A Plot of $\log vL_{v_X} - \alpha_{rx}$ for the total sample (upper left graph), HBLs (upper right graph), LBLs (lower left graph) and FSRQs (lower right graph). The empty circles represent HBLs, empty triangles LBLs and stars FSRQs. The vertical dashed line is $\alpha_{rx} = 0.75$. The oblique solid lines are the regression lines: $\log vL_{v_X} = (-5.941 \pm 0.551)\alpha_{rx} + 49.002 \pm 0.338$ for 118 HBLs, $\log vL_{v_X} = (-2.163 \pm 1.299)\alpha_{rx} + 47.129 \pm 1.010$ for 60 LBLs, and $\log vL_{v_X} = (-3.525 \pm 1.455)\alpha_{rx} + 49.230 \pm 1.264$ for 60 FSRQs.

4 DISCUSSION AND CONCLUSIONS

We have studied the correlations of $J - H$, $H - K$ and $J - K$ for HBLs, LBLs and FSRQs and found that HBLs are significantly different from LBLs and FSRQs, while there is no significant difference between LBLs and FSRQs. Besides the strong correlations between $(J - H)$ and $(J - K)$ and between $(H - K)$ and $(J - K)$ that were found in HBLs only, there is also a strong anti-correlation between the color indices $J - H$ and $H - K$, which is found only in HBLs, but is not found in either LBLs or FSRQs.

We computed the near-infrared composite spectral indices and found the average composite spectral index of HBLs is smaller than those of LBLs and FSRQs, which means that the near-infrared spectrum of HBLs are flatter than those of LBLs and FSRQs. Through the K-S test and Student's t-test, we found that the distribution and mean of the near-infrared composite spectral indices of HBLs are significantly different from those of LBLs and FSRQs, while LBLs do not differ significantly from FSRQs.

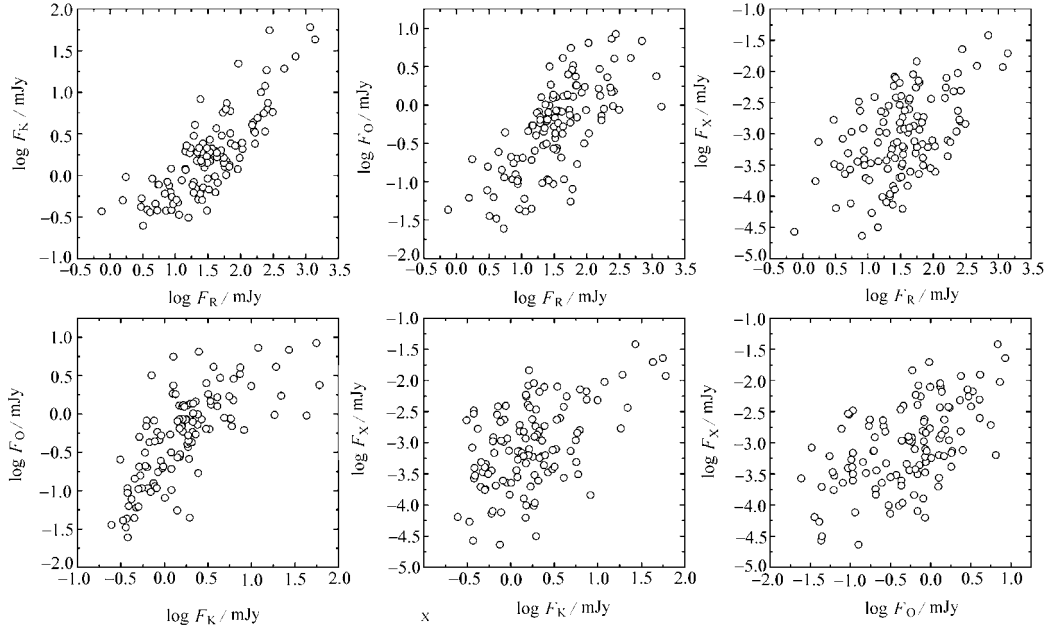


Fig. 7 Multi-wavelength flux correlations of 118 HBLs.

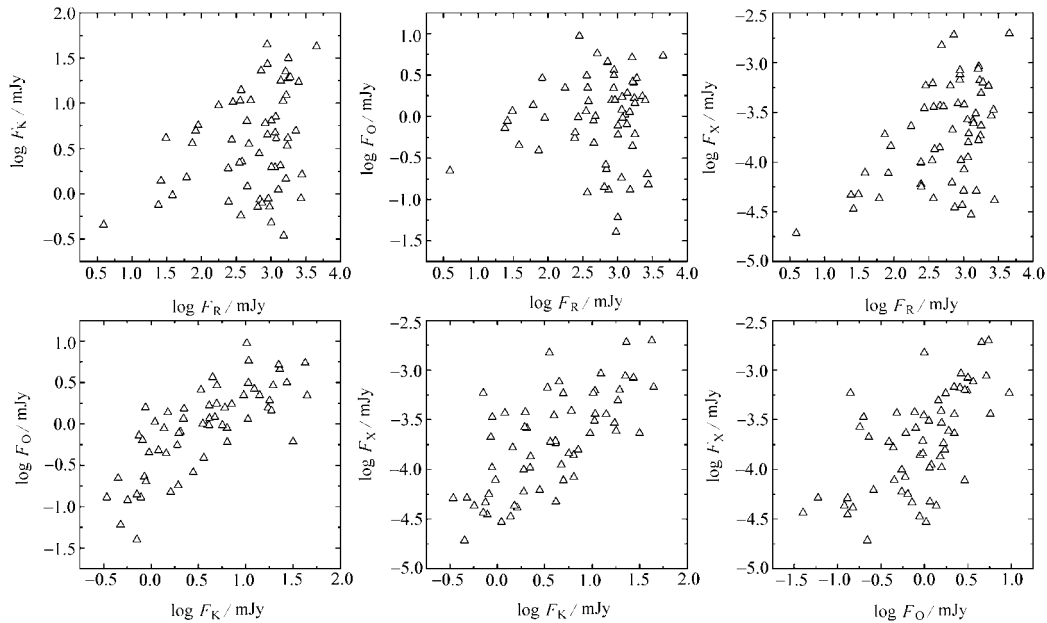


Fig. 8 Multi-wavelength flux correlations of 60 LBLs.

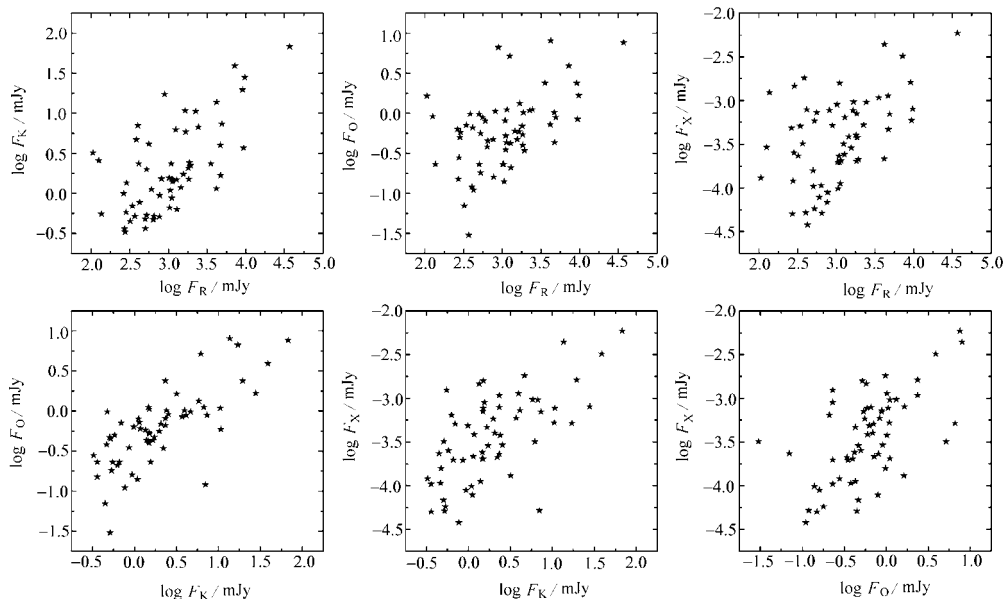


Fig. 9 Multi-wavelength flux correlations of 60 FSRQs.

We also computed K_s -band luminosities of the three subclasses and found that the averaged K_s -band luminosity of HBLs is less than those of LBLs and FSRQs, with the FSRQs a little more luminous than the LBLs. This result provides support for the argument that RBLs (LBLs) are intermediate between XBLs (HBLs) and FSRQs, and accords with the results of Sambruna et al. (1996) and Fossati et al. (1997, 1998). They found that the radio luminosity and bolometric luminosity of HBLs are lower than those of LBLs.

In several models of BL Lac emission, electromagnetic radiation is produced via synchrotron emission, by electrons possibly located in different regions and characterized by different energy distributions (Ghisellini & Maraschi 1989), from radio up to a maximum frequency generally located between the optical and the X-ray band. Above this frequency the spectrum steepens considerably because of energy losses. Substantial emission at higher energies would be still possible via inverse Compton or other mechanisms. The strong correlations between radio, near-infrared, optical and soft X-ray fluxes for HBLs in our work imply that different parts of the electromagnetic spectrum of HBLs are directly related, supporting those emission models in which radiation at different frequencies is generated by processes that are not independent. However, the situation appears more complicated and different in the case of LBLs. There are no correlations between the radio flux, and optical flux and between the radio flux and near-infrared flux and there is a weak correlation between radio flux and averaged soft X-ray flux. Such results have also been found by Giommi et al. (1990). The relativistic beaming model (Rees 1966, 1967) is generally accepted for interpreting the superluminal motion (Pearson & Zensus 1987). The enhancement of the observed fluxes due to beaming is δ^p , with $p = 3 + \alpha$ in the case of a moving sphere and $p = 2 + \alpha$ in the case of a continuous jet, where δ is the Doppler factor and the source is assumed to have a power-law spectrum. According to the synchrotron emission mechanism, one may expect a correlation between the radio and near-infrared, optical and even soft X-ray fluxes, which was confirmed by Maccagni et al. (1989) in the case of XBLs. However, in the

Table 4 Linear regression analysis results ($y = a + bx$), r denotes the Pearson's coefficient and p the chance probability.

| x | y | N | a | b | r | p | Type |
|------------|------------|-----|--------|-------|-------|-------------------------|-------|
| $\log F_R$ | $\log F_K$ | 118 | -0.792 | 0.673 | 0.808 | 2.329×10^{-28} | HBLs |
| | | 60 | -0.257 | 0.297 | 0.325 | 1.139×10^{-2} | LBLs |
| | | 60 | -1.779 | 0.685 | 0.642 | 3.334×10^{-8} | FSRQs |
| $\log F_R$ | $\log F_O$ | 118 | -1.357 | 0.701 | 0.707 | 3.522×10^{-19} | HBLs |
| | | 60 | -0.224 | 0.064 | 0.075 | 0.567 | LBLs |
| | | 60 | -1.620 | 0.462 | 0.494 | 5.922×10^{-5} | FSRQs |
| $\log F_R$ | $\log F_X$ | 118 | -3.985 | 0.613 | 0.538 | 3.354×10^{-10} | HBLs |
| | | 60 | -4.801 | 0.395 | 0.477 | 1.161×10^{-4} | LBLs |
| | | 60 | -4.900 | 0.481 | 0.486 | 8.355×10^{-5} | FSRQs |
| $\log F_K$ | $\log F_O$ | 118 | -0.489 | 0.855 | 0.719 | 4.514×10^{-20} | HBLs |
| | | 60 | -0.440 | 0.706 | 0.758 | 2.396×10^{-12} | LBLs |
| | | 60 | -0.410 | 0.642 | 0.733 | 2.712×10^{-11} | FSRQs |
| $\log F_K$ | $\log F_X$ | 118 | -3.218 | 0.710 | 0.519 | 1.702×10^{-9} | HBLs |
| | | 60 | -4.066 | 0.618 | 0.684 | 1.729×10^{-9} | LBLs |
| | | 60 | -3.620 | 0.594 | 0.641 | 3.432×10^{-8} | FSRQs |
| $\log F_O$ | $\log F_X$ | 118 | -2.866 | 0.646 | 0.561 | 3.826×10^{-11} | HBLs |
| | | 60 | -3.694 | 0.585 | 0.603 | 3.516×10^{-7} | LBLs |
| | | 60 | -3.306 | 0.627 | 0.592 | 6.257×10^{-7} | FSRQs |

case where Doppler-boosting is obvious, the correlation may be ruined. Especially in the case of RBLs (LBLs), Doppler boosting plays a very important role (Xie et al. 1991a, 1991b, 1993). On the other hand, XBLs (HBLs) are expected to be randomly oriented and the radio and optical fluxes should exhibit lower relativistic Doppler enhancement (Maraschi et al. 1986). Thus, their observed fluxes should not be very different from their intrinsic fluxes. So, during our research of the flux correlation without Doppler correction, there are still strong correlations between radio, near-infrared, optical and soft X-ray fluxes as synchrotron emission mechanism implies for HBLs (XBLs), but there are no or only weak correlations between radio and other band fluxes by reason of strong Doppler boosting effect for LBLs (RBLs). We believe for RBLs (LBLs) those strong intrinsic correlations between radio and optical and near-infrared will appear after the Doppler correction of the fluxes (Mei et al. 1999). In our study of the multi-wave band correlations, we found that the near-infrared (K_s band) flux is very strongly correlated with the optical flux, which implies that the near-infrared emission chiefly originates from synchrotron emission, and the thermal component from the dust or disk does not dominate the synchrotron emission.

We have studied the luminosity and the composite spectral index α_{rx} and found that the radio luminosity can distinguish HBLs and LBLs well but the near-infrared, optical and X-ray luminosities cannot. Our result supports the result of Mei et al. (2002) that radio luminosity can be used as a classificatory criterion of BL Lacertae objects. Moreover, we found that the radio luminosity can also distinguish HBLs and FSRQs well. In addition, we found HBLs are different from LBLs and FSRQs in the correlation between X-ray luminosity and the composite spectral index α_{rx} : for HBLs there is a very strong negative correlation between the X-ray luminosity and

the composite spectral index α_{rx} , but there is no correlation between them for LBLs and only a weak one for FSRQs. This is probably caused by the different origin mechanisms for HBLs and LBLs. The X-ray emission of HBLs is mainly due to the synchrotron process and that of LBLs is dominated by inverse Compton scattering of the same photons of the synchrotron emission. The facts above show that the continuum emission of blazars can be essentially characterized by the luminosity and suggest that the spectral shape is fundamentally connected to the luminosity. By this token, luminosity is a very important parameter and even essential one for the several parameters of blazars.

In this article, we have collected a large blazar sample including infrared data, done some statistical work on it and compared the physical properties of HBLs, LBLs and FSRQs from five aspects. The main conclusion is that HBLs are significantly different from LBLs and FSRQs, while LBLs share many properties and parameters with FSRQs. We do think that HBLs and LBLs are two kinds of blazar having different intrinsic properties and our conclusion strongly supports the suggestion of Padovani & Giommi (1995) that the classification of HBLs and LBLs is much better and has more physical significance than the classification of XBLs and RBLs.

This research made use of data products from the Two Micron All Sky Survey, which is a joint project of the University of Massachusetts and the Infrared Processing and Analysis Center/California Institute of Technology, funded by the National Aeronautics and Space Administration and the National Science Foundation. This research also made use of NASA/IPAC Extragalactic Database (NED), which is operated by the Jet Propulsion Laboratory, California Institute of Technology, under contract with the National Aeronautics and Space Administration.

References

- Angle J. R. P., Stockman H. S., 1980, *ARA&A*, 18, 321
Baker J., 1997, *MNRAS*, 286, 23
Bondi M., Marchã M. J. M., Dallacasa D. et al., 2001, *MNRAS*, 325, 1109
Böttcher M., Dermer C. D., 2002, *ApJ*, 564, 86
Bregman J. N., Glassgold A. E., Huggins P. J. et al., 1990, *ApJ*, 352, 574
Brinkmann W., Siebert J., Reich W. et al., 1995, *A&AS*, 109, 147
Comastri A., Molendi S., Ghisellini G., 1995, *MNRAS*, 277, 297
Comastri A., Fossati G., Ghisellini G. et al., 1997, *ApJ*, 480, 534
D'Elia V., Cavalitre A., 2001, *ASP Conference Series*, 227, 252
Donato D., Ghisellini G., Tagliaferri G. et al., 2001, *A&A*, 375, 739
Dong Y. M., Mei D. C., Liang E. W., 2002, *PASJ*, 54, 171
Falomo R., Bersanelli M., Bouchet P. et al., 1993, *AJ*, 106, 11
Fan J. H., Xie G. Z., Lin R. G. et al., 1998, *A&AS*, 133, 217
Fan J. H., Lin R. G., 1999, *ApJS*, 121, 131
Fossati G., Celotti A., Ghisellini G. et al., 1997, *MNRAS*, 289, 136
Fossati G., Maraschi L., Celotti A. et al., 1998, *MNRAS*, 299, 433
Fugmann W. 1988, *A&A*, 205, 86
Gear W. K., 1993, *MNRAS*, 264, 919
Ghisellini G., Maraschi L., 1989, *ApJ*, 340, 181
Giommi P., Barr P., Pollock A. M. T. et al., 1990, *ApJ*, 356, 432
Giommi P., Padovani P., 1994, *MNRAS*, 268, 51
Lamer G., Brunner H., Staubert R. et al., 1996, *A&A*, 311, 384
Ledden J. E., O'Dell S. L., 1985, *ApJ*, 298, 630
Maccagni D. et al., 1989, In: Maraschi L., Maccacaro T., Ulirich M. H. eds., *BL Lacertae Objects, Lecture Notes in Physics*, 334, Berlin: Springer, p.281

- Maraschi L., Ghisellini G., Tanzi E. G. et al., 1986, *ApJ*, 310, 325
Maraschi L., Rovetti F., 1994, *ApJ*, 436, 79
Maraschi L., Fossati G., Tagliaferri G. et al., 1995, *ApJ*, 443, 578
Mei D. C., Xie G. Z., Qin Y. P. et al., 1999, *PASJ*, 51, 579
Mei D. C., Zhang L., Jiang Z. J. et al., 2002, *A&A*, 391, 917
Padovani P., 1992, *MNRAS*, 257, 404
Padovani P., Giommi P., 1995, *ApJ*, 444, 567
Padovani P., 1999, *ASP Conference Series*, 159, 339
Pearson T. J., Zensus J. A., 1987, In: J. A. Zensus, T. J. Pearson, eds., *Superluminal Radio Source*, Cambridge: Cambridge Univ. Press, p.1
Perlmutter S., Stocke J. T., Schachter J. F. et al., 1996, *ApJS*, 104, 251
Press W. H., Teukolsky S. A., Vetterling W. T., Flannery B. P., 1992, In: *Numerical Recipes in Fortran, The Art of Scientific Computing* (2nd ed.) Cambridge: Cambridge Univ. Press
Qin Y. P., Xie G. Z., Zheng X. T., 1999, *Ap&SS*, 266, 549
Rees M. J., 1966, *Nature*, 211, 468
Rees M. J., 1967, *MNRAS*, 135, 345
Sambruna R. M., Maraschi L., Urry C. M. et al., 1996, *ApJ*, 463, 444
Sillanpaa A., Takalo L. O., Kikuchi S. et al., 1991, *AJ*, 101, 2017
Stecker F. W., de Jager O. C., Salamon M. H. et al., 1996, *ApJ*, 473, 75
Skrutskie M. F. et al., 1997, In: F. Garzon et al. eds., *The Impact of Large Scale Near-IR Sky Surveys*, Dordrecht: Kluwer, p.25
Urry C. M., Padovani P., 1995, *PASP*, 107, 803
Vagnetti F., Cavaliere A., Giallongo E., 1991, *ApJ*, 368, 366
Voges W., Aschenbach B., Boller T. et al., 1996, *IAUC*, 6420
Webster R. L., Francis P. J., Peterson B. A. et al., 1995, *Nature*, 375, 469
Wills B. J., Hines D. C., 1997, In: N. Arav, I. Shlosman, R. J. Weymann, *Mass Ejection from Active Galactic Nuclei*, San Francisco: ASP, p.99
Wolter A., Comastri L., Ghisellini L., 1998, *A&A*, 335, 396
Xie G. Z., Li K. H., Cheng F. Z. et al., 1991a, *A&AS*, 87, 461
Xie G. Z., Liu F. K., Liu B. F. et al., 1991b, *A&A*, 249, 65
Xie G. Z., Zhang Y. H., Fan J. H. et al., 1993, *A&A*, 278, 6
Xie G. Z., Dai B. Z., Liang E. W. et al., 2001a, *PASJ*, 53, 469
Xie G. Z., Dai B. Z., Mei D. C. et al., 2001b, *ChJAA*, 1, 213
Xie G. Z., Ding S. X., Dai H. et al., 2003, *IJMPD*, 12, 781
Xie G. Z., Zhou S. B., Li K. H. et al., 2004a, *MNRAS*, 348, 831
Xie G. Z., Zhou S. B., Liu H. T. et al., 2004b, *IJMPD*, 13, 347
Xie G. Z., Ma L., Liang E. W. et al., 2004c, *AJ*, 126, 2108